Synthesis, Molecular Structures, and Dynamics of Primary and Secondary Fluoroalkyl Complexes of Palladium(II) with Tetramethylethylenediamine (TMEDA) Ligands. Evaluation of the Structural *trans*-Influences of Methyl and Fluoroalkyl Groups as Ligands within the Same Coordination Sphere

Russell P. Hughes,*,† Jason S. Overby,† Alex Williamson,† Kin-Chung Lam,‡ Thomas E. Concolino,‡ and Arnold L. Rheingold‡

Departments of Chemistry, 6128 Burke Laboratory, Dartmouth College, Hanover, New Hampshire 03755, and University of Delaware, Newark, Delaware 19716

Received August 10, 2000

Reaction of (TMEDA)Pd(CH_3)$_2$ (TMEDA = tetramethylethylenediamine) with primary perfluoroalkyl iodides gives a mixture of products that depend markedly on the choice of solvent. In hexanes, (TMEDA)PdMe(R_F) [R_F = *n*-C_3F_7 (**1**); *n*-C_4F_9 (**2**)] is afforded in about 50% yield, with (TMEDA)Pd(CH_3)I (**3**) formed concurrently. In hexanes **3** precipitates from solution and does not react further, but with THF as the solvent **3** remains in solution and reacts with R_FI in the presence of light to give (TMEDA)PdI(R_F) [R_F = *n*-C_3F_7 (**4**); *n*-C_4F_9 (**5**)] and (TMEDA)PdI_2, as well as **1** and **2**, respectively. Treatment of either **1** or **2** with I_2 yields the corresponding iodide compounds **4** and **5**, with elimination of CH_3I, while an analogous reaction of **2** with concentrated HCl produces the chloride compound (TMEDA)PdCl(C_4F_9) (**8**). In contrast, reaction of (TMEDA)Pd(CH_3)$_2$ with the secondary iodide ICF(CF_3)$_2$ gives only one fluoroalkyl product, (TMEDA)Pd(CH_3)(*i*-C_3F_7) (**6**), in either hexanes or THF. Reaction of **6** with I_2 occurs with selective cleavage of the Pd−CH_3 bond to give the iodide product (TMEDA)PdI(*i*-C_3F_7) (**7**). The solid-state structures of **1**−**5**, **7**, and **8** have been confirmed by X-ray crystallography. Examination of bond distances illustrates that fluoroalkyl ligands have smaller *trans*-influences than methyl ligands, but larger *trans*-influences than iodide or chloride ligands toward the N-donor TMEDA ligand. This results in a shorter, presumably stronger Pd−fluoroalkyl bond being *trans* to a shorter, presumably stronger Pd−N bond. The principal steric effect of the perfluoroisopropyl group in the solid state is to generate an almost planar TMEDA ring. The solution NMR data for **1**, **2**, **4**, **5**, and **8** show resonances due to diastereotopic CF_2 groups below room temperature, with the CF_2 group acting as a remote sensor for formation of a stereocenter at the metal due to slowing of the inversion of the puckered five-membered metallacycle formed by the TMEDA ligand and Pd. The other TMEDA complexes show the same behavior below room temperature, with the exception of (TMEDA)PdI(*i*-C_3F_7) (**7**), in which the TMEDA ring is presumably almost planar in the ground state.

Introduction

Oxidative addition and reductive elimination reactions are two of the fundamental pathways of reactivity in organometallic complexes.[1] Oxidative addition reactions of alkyl halides are among the most useful in forming new metal−carbon bonds. There has been a recent renaissance of interest in transition metal complexes containing fluoroalkyl ligands. While many such compounds have been prepared using oxidative addition methodology,[2−7] the fluoroalkyl ligand was usually found to be inert chemically and thermally, and these compounds were often relegated to footnotes when compared with their much more reactive and industrially important hydrocarbon analogues. However, recent work has shown that fluoroalkyl ligands are indeed reactive under quite mild conditions, and examples of F-migrations to and from metal centers[8] and activation

* Corresponding author. E-mail address: rph@dartmouth.edu. Fax: (603) 646-3946.
† Dartmouth College.
‡ University of Delaware.

(1) Collman, J. P.; Hegedus, L. S.; Norton, J. R.; Finke, R. G. *Principles and Applications of Organotransition Metal Chemistry*; University Science Books: Mill Valley, CA, 1987.
(2) McCleverty, J. A.; Wilkinson, G. *J. Chem. Soc.* **1964**, 4200−4203.
(3) Rosevear, D. T.; Stone, F. G. A. *J. Chem. Soc. A* **1968**, 164−167.
(4) Mukhedkar, A. J.; Green, M.; Stone, F. G. A. *J. Chem. Soc. A* **1969**, 3023−3026.
(5) Stone, F. G. A. *Endeavour* **1966**, *25*, 33−38.
(6) Clark, H. C.; Manzer, L. E. *J. Organomet. Chem.* **1973**, *59*, 411−428.
(7) Appleton, T. G.; Hall, J. R.; Kennard, C. H. L.; Mathieson, M. T.; Neale, D. W.; Smith, G.; Mak, T. C. W. *J. Organomet. Chem.* **1993**, *453*, 299−306.
(8) Huang, D.; Caulton, K. G. *J. Am. Chem. Soc.* **1997**, *119*, 3185−3186.

10.1021/om000694k CCC: $19.00
Publication on Web 11/03/2000

of carbon−fluorine bonds by hydrolysis[9] and hydrogenolysis[10] have been observed.

Consequently we have been interested in reevaluating and expanding some previously reported methodology for the synthesis of late metal−fluoroalkyl complexes. The most common method used is that of oxidative addition of a fluoroalkyl iodide to a low-valent metal center, although we have shown previously that this method is often fraught with complications due to fluoroalkylation at ligand sites, rather than at the metal center.[11−13]

We were interested in preparing some fluoroalkyl complexes of palladium(II) to evaluate their chemical reactivity and were cognizant of literature reports that Pd(0) and Pt(0) phosphine complexes ML_4 underwent oxidative addition with a wide variety of perfluoroalkyl halides to give the corresponding divalent perfluoroalkyl halide compounds *trans*-ML_2R_FI.[3,4] However, in our hands these reactions are at best difficult to repeat and are consistently plagued by the concurrent formation of the metal dihalide complexes ML_2I_2 in varying yields. Another preparation of such complexes was successful when gaseous palladium atoms were allowed to cocondense with vapors of perfluoroalkyl iodides.[14] While these complexes are reported to be remarkably stable, this route is of less synthetic utility.

Besides oxidative addition to zerovalent metal complexes, such reactions can also be accomplished with divalent complexes of platinum. It had been shown previously that (COD)Pt$(CH_3)_2$ could serve as a precursor to perfluoroalkyl complexes as the Pt(II) complex would undergo oxidative addition with CF_3I to give (COD)Pt$(CF_3)_2$ with $[Pt(CH_3)_3I]_4$ as a byproduct.[6] Likewise, (NBD)Pt$(CH_3)_2$ (NBD = norbornadiene) reacted under similar reactions with CF_3I, and (NBD)Pt(CH_3)-(CF_3) and (NBD)Pt$(CF_3)_2$ could be isolated from the reaction mixtures.[7,15−20] Larger perfluoroalkyl iodides (e.g., perfluoroethyl, perfluoropropyl, perfluoroisopropyl) also appeared to form stable Pt(II) complexes, although none could be isolated in pure form.[6] All these products were presumed to result from oxidative addition of the perfluoroalkyl iodide to Pt(II), followed by reductive elimination of MeI from a Pt(IV) intermediate.

We reasoned that dimethylpalladium(II) compounds should give comparable results and settled upon (TMEDA)Pd$(CH_3)_2$ (TMEDA = *N*,*N*,*N*′,*N*′-tetramethylethylenediamine) as a suitable precursor. This complex has been demonstrated to oxidatively add a variety of organic substrates, forming Pd(IV) intermediates that decompose at ambient temperature by reductive elimination to provide new, stable Pd(II) complexes.[21,22] In addition, TMEDA complexes of platinum, (TMEDA)Pt-$(CH_3)(CF_3)$ and (TMEDA)Pt$(CF_3)_2$, analogous to the desired palladium products, have been isolated by displacement of NBD from (NBD)Pt$(CH_3)(CF_3)$ and (NBD)Pt$(CF_3)_2$.[7,20]

Results and Discussion

Synthesis of Perfluoroalkyl Palladium Complexes. When primary perfluoroalkyl iodides, R_FI, (R_F = *n*-C_3F_7, *n*-C_4F_9) were added to a hexanes suspension of (TMEDA)Pd$(CH_3)_2$, two products were formed in approximately equal amounts. Filtration and extraction of the precipitate with hexanes afforded the pale yellow complexes (TMEDA)Pd$(CH_3)(R_F)$ (*n*-C_3F_7, **1**; *n*-C_4F_9, **2**) as air and moisture stable solids. Their ^{19}F NMR spectra were consistent with the proposed structures, and in addition, both compounds were characterized by single-crystal X-ray diffraction studies (see below). The hexanes-insoluble material was determined to be (TMEDA)-Pd$(CH_3)I$ (**3**), initially identified by its previously reported ^1H NMR spectrum[21] and subsequently confirmed by an X-ray diffraction study (see below). The formation of both **1** and **2** is readily rationalized by initial oxidative addition of the fluoroalkyl iodide to (TMEDA)Pd$(CH_3)_2$ to give the putative Pd(IV) intermediate (TMEDA)Pd-$(CH_3)_2I(R_F)$, followed by reductive elimination of MeI. Subsequent oxidative addition of the MeI to the starting material (TMEDA)Pd$(CH_3)_2$ followed by reductive elimination of ethane gives (TMEDA)Pd$(CH_3)I$ (**3**), as reported previously,[21] Thus, competition of liberated MeI with R_FI for the (TMEDA)Pd$(CH_3)_2$ starting material clearly appears to limit the yield of fluoroalkyl complexes **1** and **2** under these conditions.

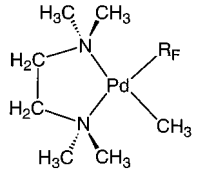

1 $R_F = CF_2CF_2CF_3$
2 $R_F = CF_2CF_2CF_2CF_3$

In contrast, when a solution of (TMEDA)Pd$(CH_3)_2$ in THF was allowed to react with the same primary fluoroalkyl iodides, two fluoroalkyl compounds were isolated upon removal of the reaction solvent and washing with hexanes. The hexanes extract was shown to contain the previously observed fluoroalkyl(methyl) complexes **1** and **2**, while the corresponding fluoroalkyl(iodo) complexes (TMEDA)PdI(R_F) (*n*-C_3F_7, **4**; *n*-C_4F_9, **5**) were recovered as hexane-insoluble, pale orange, air and moisture stable solids. In addition variable amounts of

(9) Hughes, R. P.; Lindner, D. C.; Rheingold, A. L.; Liable-Sands, L. M. *J. Am. Chem. Soc.* **1997**, *119*, 11544−11545.
(10) Hughes, R. P.; Smith, J. M. *J. Am. Chem. Soc.* **1999**, *121*, 6084−6085.
(11) Hughes, R. P.; Husebo, T. L.; Holliday, B. J.; Rheingold, A. L.; Liable-Sands, L. M. *J. Organomet. Chem.* **1997**, *548*, 109−112.
(12) Hughes, R. P.; Maddock, S. M.; Rheingold, A. L.; Liable-Sands, L. M. *J. Am. Chem. Soc.* **1997**, *119*, 5988−5989.
(13) Hughes, R. P.; Husebo, T. L.; Rheingold, A. L.; Liable-Sands, L. M.; Yap, G. P. A. *Organometallics* **1997**, *16*, 5−7.
(14) Klabunde, K. J.; Campostrini, R. *J. Fluorine Chem.* **1989**, *42*, 93−104.
(15) Appleton, T. G.; Bennett, M. A. *Inorg. Chem.* **1978**, *17*, 738−747.
(16) Appleton, T. G.; Hall, J. R.; Neale, D. W.; Williams, M. A. *J. Organomet. Chem.* **1984**, *276*, C73−C76.
(17) Appleton, T. G.; Hall, J. R.; Williams, M. A. *J. Organomet. Chem.* **1986**, *303*, 139−149.
(18) Appleton, T. G.; Berry, R. D.; Hall, J. R.; Neale, D. W. *J. Organomet. Chem.* **1988**, *342*, 399−422.
(19) Appleton, T. G.; Berry, R. D.; Hall, J. R.; Neale, D. W. *J. Organomet. Chem.* **1989**, *364*, 249−273.
(20) Appleton, T. G.; Hall, J. R.; Mathieson, M. T.; Neale, D. W. *J. Organomet. Chem.* **1993**, *453*, 307−316.
(21) Graaf, W. d.; Boersma, J.; Smeets, W. J. J.; Spek, A. L.; Koten, G. v. *Organometallics* **1989**, *8*, 2907−2917.
(22) Graaf, W. D.; Boersma, J.; Koten, G. V. *Organometallics* **1990**, *9*, 1479−1484.

the diiodo complex (TMEDA)PdI_2 were observed in this reaction.

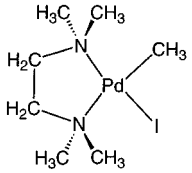

3

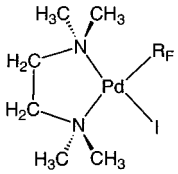

4 $R_F = CF_2CF_2CF_3$
5 $R_F = CF_2CF_2CF_2CF_3$

The effects of solvent on product outcome in reductive elimination reactions from Pt(IV) intermediates has been the subject of detailed studies, and changes in mechanism resulting from differing solvent polarities have been demonstrated.[23,24] However, in our reactions the cause of the product variation in hexanes and THF appears be more mundane, seemingly a result of the insolubility of **3** in hexanes, which precludes its further reaction with R_FI. In a separate experiment, treatment of **3** with *n*-C_3F_7I in THF results in conversion to **4**, with elimination of MeI and formation of (TMEDA)PdI_2 as a byproduct. Thus in hexanes, precipitation of **3** removes it from solution, and subsequent reaction to form **4** is not observed. The reaction is, however, even more complicated. *The reaction of (TMEDA)Pd(CH_3)I (**3**) with n-C_3F_7I in THF does not occur in the dark, but the reaction of (TMEDA)Pd(CH_3)$_2$ does!* Consequently, when the reaction of (TMEDA)Pd(CH_3)$_2$ with *n*-C_3F_7I in THF is carried out in the dark, the products are **1** (54%) and **3** (44%), with no traces of **4** or (TMEDA)PdI_2.

Treatment of isolated **4** with CH_3MgBr affords **1**. *Consequently the best way to prepare the fluoroalkyl(methyl) complex **1** in high yield is to carry out the reaction of (TMEDA)Pd(CH_3)$_2$ with n-C_3F_7I in THF to give a mixture of **1** and **4**, followed by treatment of the mixture with 0.5 equiv of CH_3MgBr to convert **4** to **1**.* This method affords **1** in 91% yield.

In further contrast, reaction of (TMEDA)Pd(CH_3)$_2$ with the secondary fluoroalkyl iodide ICF(CF_3)$_2$ afforded the fluoroalkyl(methyl) complex (TMEDA)Pd(CH_3)(*i*-C_3F_7) (**6**), regardless of whether the solvent was hexanes or THF. In hexanes, the insoluble **3** is also formed, while in THF the principal byproduct is the diiodide (TMEDA)-PdI_2. We have not explored this reaction further or optimized the conditions. It is proposed that the byproduct, CH_3I, formed by reaction of (TMEDA)Pd(CH_3)$_2$ with *i*-C_3F_7I, reacts with remaining (TMEDA)Pd(CH_3)$_2$ to give (TMEDA)Pd(CH_3)I (**3**). This compound then reacts with *i*-C_3F_7I to give (TMEDA)PdI_2. As predicted by this hypothesis, **3** reacts with *i*-C_3F_7I in THF to produce (TMEDA)PdI_2. The fate of the fluoroalkyl group not incorporated into the coordination sphere of palladium was found to be (CF_3)$_2$CFH, identified by its NMR spectra and by gas chromatography/mass spectrometry.

Compounds **1**, **2**, and **6** showed no reaction with additional equivalents of perfluoroalkyl iodide or methyl iodide, indicating that once formed, they are inert to oxidative addition of this type of C−I bond. This is in contrast to the behavior apparently exhibited by (NBD)-Pt(CH_3)(CF_3), which is presumed to undergo a subsequent oxidative addition reaction with excess CF_3I, followed by elimination of MeI to give the homoleptic perfluoroalkyl species (NBD)Pt(CF_3)$_2$.[7] However, elemental I_2 reacts cleanly with **1**, **2**, and **6** to yield the corresponding fluoroalkyl(iodo) complexes **4**, **5**, and **7**, respectively. Complexes **4**, **5**, and **7** show air and moisture stability analogous with that seen for their precursors. Compound **2** also reacts with concentrated aqueous HCl to yield the chloride complex (TMEDA)-Pd($CF_2C_4F_9$) (**8**) as an air and moisture stable crystalline solid. In view of previous observations in our laboratories and by others, it is noteworthy that there is no acid-promoted hydrolysis of the α-CF_2 group under these conditions.

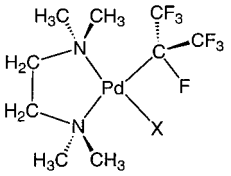

6 X = CH_3
7 X = I

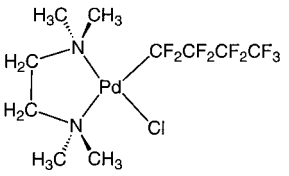

8

^{19}F NMR Spectra of the Fluoroalkyl Complexes. While the structures of these fluoroalkyl complexes have been unambiguously confirmed by X-ray crystallography (see below), the ^{19}F NMR spectra of the *n*-fluoroalkyl compounds provided some surprises. At room temperature, the fluoroalkyl(methyl) complexes **1** and **2** exhibited the appropriate number of ^{19}F resonances for their respective fluoroalkyl groups, although that of the α-CF_2 was broad. At first sight, the corresponding NMR spectra of the halide analogues **4**, **5**, and **8** were remarkable in that the expected resonance for the α-CF_2 group was missing from the spectrum in each case. This apparently unusual solution phenomenon was investigated further by variable-temperature ^{1}H and ^{19}F NMR spectroscopy. Figure 1 illustrates the changes observed in the ^{19}F NMR spectrum of a toluene-d_8 solution of the perfluoro-*n*-butyl(iodo) complex **5** as the temperature is changed. At 20 °C only three signals are observed, assignable to the β-CF_2, γ-CF_2, and CF_3 groups, as shown. At 80 °C the resonance of the α-CF_2 group is apparent at δ −74.69 ppm. On progressive cooling from 20 to −60 °C the resonances of the α-CF_2 fluorines appear as an AX system, eventually appearing as strongly coupled ($J_{F\alpha\alpha'}$ = 240 Hz) doublets at δ −58.75 and −94.24 ppm; in addition the resonances of the β and γ-CF_2 fluorines broaden and decoalesce into AB quartets at δ −107.74 and −109.34 ppm ($J_{F\beta\beta'}$ = 289 Hz) and δ −124.25 and −128.34 ppm ($J_{F\gamma\gamma'}$ = 289 Hz), respectively. Clearly at low temperature the ground-state conformation of this complex is such as to render all fluorines in CF_2 groups diastereotopic; that is, the remainder of the complex must contain a stereocenter, generating a very large ∼35.5 ppm chemical shift difference between the two diastereotopic α-fluorines close to the stereocenter, and progressively smaller chemical shift differences within the β- and γ-CF_2 groups. As the temperature is raised, rapid epimerization of the stereocenter causes pairwise coalescence of the diastereotopic resonances. Consequently the "missing" resonance of the α-CF_2 group at 20 °C is due to the

(23) Goldberg, K. I.; Yan, J. Y.; Winter, E. L. *J. Am. Chem. Soc.* **1994**, *116*, 1573−1574.
(24) Goldberg, K. I.; Yan, J.; Breitung, E. M. *J. Am. Chem. Soc.* **1995**, *117*, 6889−6896.

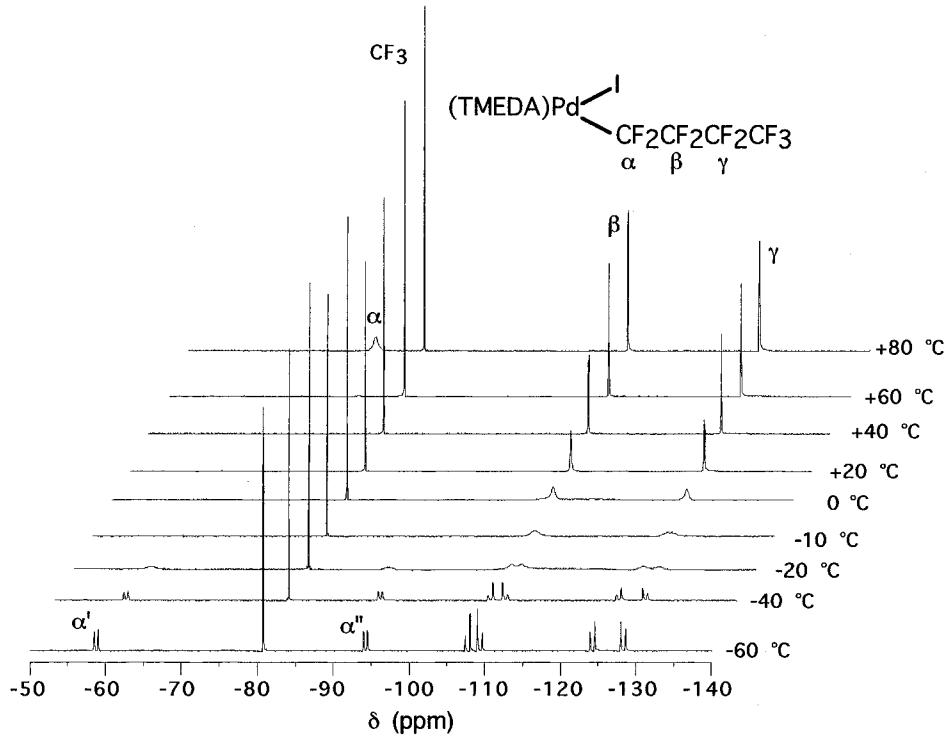

Figure 1. Variable-temperature ^{19}F NMR spectra of (TMEDA)PdI(C_4F_9), **5**. In the −60° spectrum α′ and α″ denote the fluorine resonances on the α-CF_2 that are completely coalesced at +20 °C.

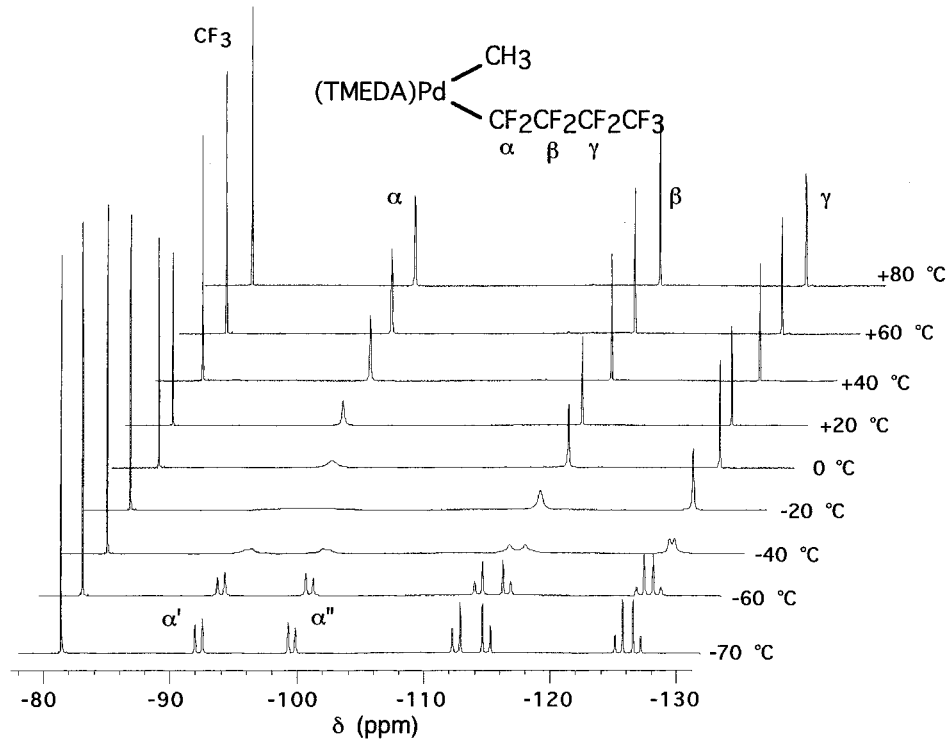

Figure 2. Variable-temperature ^{19}F NMR spectra of (TMEDA)Pd(CH_3)(C_4F_9), **2**.

fact that at this temperature the resonances of these fluorines are so broad as to disappear into the baseline, yet those of the β- and γ-CF_2 groups have already reached coalescence at 20 °C. Analogous behavior is observed in the ^{19}F spectra of **4** and **8**.

The corresponding variable-temperature ^{19}F NMR spectra of **2**, the methyl analogue of **5**, are shown in Figure 2 and contain the same features as those observed for **5**. In this case the low-temperature spectrum illustrates the same diastereotopic nature of each fluorine within each CF_2 group; the notable difference is that the chemical shift difference of the diastereotopic α-CF_2 fluorines is approximately 7.3 ppm, compared with 36 ppm in **5**. Because of the much smaller chemical shift difference, coalescence of these resonances occurs at a much lower temperature in **2** compared to **5**, and at room temperature the spectrum of **2** appears as originally expected, albeit with a somewhat broadened

Table 1. Crystal Data and Summary of X-ray Data Collection[a]

	1	**4**	**2**	**8**	**5**	**3**	**7**
	$L_2PdMe(n\text{-}C_3F_7)$	$L_2PdI(n\text{-}C_3F_7)$	$L_2PdMe(n\text{-}C_4F_9)$	$L_2PdCl(n\text{-}C_4F_9)$	$L_2PdI(n\text{-}C_4F_9)$	L_2PdMeI	$L_2PdI(i\text{-}C_3F_7)$
formula	$C_{10}H_{19}F_7N_2Pd$	$C_9H_{16}F_7IN_2Pd$	$C_{11}H_{19}F_9N_2Pd$	$C_{10}H_{16}ClF_9N_2Pd$	$C_{10}H_{16}F_9IN_2Pd$	$C_7H_{19}IN_2Pd$	$C_9H_{16}F_7IN_2Pd$
fw	406.67	518.54	456.68	477.10	568.55	364.57	518.55
space group	$P\bar{1}$	$P\bar{1}$	$P2(1)/n$	$P2(1)/c$	$P2(1)/c$	$P2(1)/n$	$Pca2(1)$
a, Å	8.3909(2)	9.464(4)	11.884(3)	10.633(3)	10.266(4)	8.444(5	13.551(3)
b, Å	8.9938(2)	12.968(4)	11.059(2)	11.750(4)	14.254(4)	11.285(5)	8.885(5)
c, Å	20.4192(2)	13.114(5)	12.676(3)	13.497(3)	12.155(8)	12.430(7)	13.226(5)
α, deg	84.7442(5)	89.20(3)	90	90	90	90	90
β, deg	88.3415(5)	88.88(4)	95.844(13)	104.296(19)	104.17(8)	98.66(4)	90
γ, deg	80.1482(6)	78.86(2)	90	90	90	90	90
V, Å^3	1511.72(5)	1578.7(11)	1657.4(8)	1638.6(9)	1724(14)	1170.9(12)	1592.3(13)
Z	4	4	4	4	4	4	4
D(calcd), g/cm^3	1.787	2.182	1.830	1.934	2.190	2.068	2.163
abs coeff, mm^{-1}	1.293	3.193	1.207	1.383	empirical	4.175	3.166
temp, K	173(2)	267(2)	243(2)	235(2)	243(2)	249(2)	235(2)
diffractometer				Siemens P4			
radiation				Mo Kα 0.71073 Å			
$R(F)$, %[b]	7.89	5.67	4.17	3.01	6.38	4.05	5.83
$R(wF^2)$, %[b]	20.43	13.26	12.07	7.74	14.75	12.73	14.61

[a] L_2 = tetramethylethylenediamine (TMEDA). [b] Quantity minimized = $R(wF^2) = \sum[w(F_o^2 - F_c^2)^2]/\sum[(wF_o^2)^2]^{1/2}$; $R = \sum\Delta/\sum(F_o)$, $\Delta = |(F_o - F_c)|$.

α-CF_2 peak. Heating the sample simply sharpens all the resonances. Analogous behavior is observed in the ^{19}F NMR spectrum of **1**.

Though not as dramatic as the ^{19}F spectra, the variable-temperature ^1H spectra of **1**, **2**, **4**, **5**, and **8** also show behavior consistent with formation of a stereocenter at low temperatures, with rapid epimerization on the NMR time scale at room temperature and above. For example, in the case of **5** cooling the sample causes the CH_2CH_2 resonances to broaden and eventually decoalesce to four resonances at −60 °C, while the two NMe_2 resonances observed at room temperature broaden and decoalesce into three singlets, with accidental overlap of one pair of Me resonances. This ^1H and ^{19}F NMR behavior is consistent only with the slowing of the inversion process that interconverts the λ and δ conformers of the puckered TMEDA ring in each of these compounds. At low temperature a sufficiently slow inversion rate affords an effective stereocenter at the metal, which accounts for all the NMR observations. Such interconversion of puckered conformers of the TMEDA ring has been observed previously in (TMEDA)Pd$(CH_3)_2$ and in other chelating diamine complexes. The activation barriers for this process in compounds **1**, **2**, **4**, **5**, and **8** were all determined to be between 11 and 13 ± 1 kcal mol^{-1}. These values are virtually identical to the value of 10.3 kcal mol^{-1} determined for TMEDA inversion in (TMEDA)Pd$(CH_3)_2$,[21] indicating that the nature of ancillary methyl, *n*-fluoroalkyl, or halide ligands on Pd does not affect this barrier significantly.

The ^{19}F NMR spectra of the corresponding perfluoroisopropyl analogues **6** and **7** were unremarkable and did not exhibit any evidence of diastereotopic CF_3 groups due to slowing of the TMEDA ring puckering at low temperatures. The absence of such a process is due to the fact that the TMEDA ring in **7**, unlike the significantly puckered rings in all the other analogues, is actually almost planar in the solid-state structure (see below).

The slowing of inversion of TMEDA ring puckering at low temperature with generation of a stereocenter at palladium and diastereotopic environments for each pair of CF_2 fluorines affords an unexpected means of measuring the geminal F−F coupling constants; it is noteworthy that while $J_{\beta\beta'}$ and, where appropriate, $J_{\gamma\gamma'}$ are virtually constant at ∼290 Hz in every molecule, the value of $J_{\alpha\alpha'}$ is significantly smaller. For example, in the series of perfluoro-*n*-butyl complexes $J_{\alpha\alpha'}$ = 275 Hz in **2**, 240 Hz in **5**, and 230 Hz in **8**.

Solid-State Structures. To determine the structural parameters of these new types of fluoroalkyl complexes, the solid-state structures of **1**, **2**, **4**, **5**, **7**, and **8** were determined by single-crystal X-ray diffraction studies. In addition, the previously unknown solid-state structure of **3** was determined to allow for more direct comparisons between the structural parameters of perfluoroalkyl groups and methyl groups in palladium(II) complexes. Details of the crystallographic determinations are provided in Table 1, selected bond lengths are assembled in Table 2, and ORTEP drawings appear in Figures 3−9.

(TMEDA)Pd$(CH_3)(n\text{-}C_3F_7)$ (1) crystallizes in the triclinic space group $P\bar{1}$ with two crystallographically independent molecules in the unit cell. These molecules exist as an enantiomeric pair in which both molecules adopt the expected distorted square-planar geometry. An ORTEP of one molecule is shown in Figure 3, and an ORTEP showing both molecules is provided in the Supporting Information.

Relevant bond distances are provided in Table 2. It is noteworthy that the average Pd−C_F bond distance of 1.983(9) Å is smaller than the average Pd−CH_3 distance of 2.092(10) Å. The latter bond length is not significantly different from that in (TMEDA)Pd(CH_3)Ph (2.107(3) Å)[25] but larger than the average distance in (TMEDA)Pd$(CH_3)_2$ (2.027(3) Å).[21] There is also a difference in the Pd−N distances, with the average bond distance to the nitrogen *trans* to the *n*-C_3F_7 ligand significantly shorter (Pd−N(2) = 2.151(9) Å) than that *trans* to CH_3 (Pd−N(1) = 2.225(8) Å). This trend shows that the methyl ligand has a higher structural *trans*-influence than the

(25) Markies, B. A.; Canty, A. J.; Graaf, W. D.; Boersma, J.; Janssen, M. D.; Hogerheide, M. P.; Smeets, W. J. J.; Spek, A. L.; Koten, G. V. *J. Organomet. Chem.* **1994**, *482*, 191−199.

Table 2. Bond Distances to Palladium (in Å) for Perfluoroalkyl and Alkyl Complexes

compound	Pd−N(1)	Pd−N(2)	Pd−R_F	Pd−X (*trans* to N(1))	reference
1 molecule 1	2.222(8)	2.162(9)	1.996(9)	2.106(10)	this work
1 molecule 2	2.228(8)	2.139(9)	1.970(11)	2.078(10)	this work
2	2.235(4)	2.167(4)	1.990(5)	2.052(5)	this work
4 molecule 1	2.144(10)	2.166(9)	2.002(12)	2.5700(16)	this work
4 molecule 2	2.140(9)	2.164(11)	2.002(13)	2.5734(14)	this work
5	2.136(17)	2.175(11)	1.943(17)	2.5824(17)	this work
7	2.126(17)	2.137(18)	2.02(2)	2.588(2)	this work
8	2.103(4)	2.143(4)	2.002(5)	2.2951(13)	this work
3[a]	2.120(7)	2.204(7)	2.152(7)	2.5760(14)	this work
(TMEDA)Pd(CH_3)$_2$	2.200(2)	2.197(2)	2.026(3)	2.029(3)	21
(TMEDA)PdPhI[b]	2.127(6)	2.193(6)	1.992(7)	2.5703(8)	25
(TMEDA)Pd(CH_3)Ph[c]	2.195(3)	2.210(3)	2.107(3)	1.985(3)	25

[a] R = Me; X = I. [b] R = Ph, X = I. [c] R = Me, X = Ph.

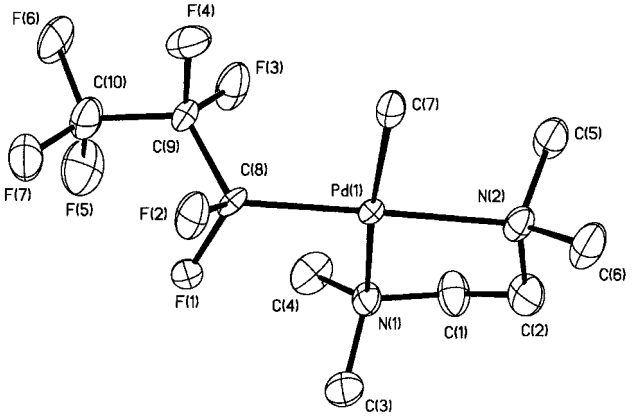

Figure 3. ORTEP diagram of the non-hydrogen atoms of (TMEDA)Pd(CH_3)(*n*-C_3F_7) (**1**), showing atom-labeling scheme. Thermal ellipsoids are shown at the 30% level.

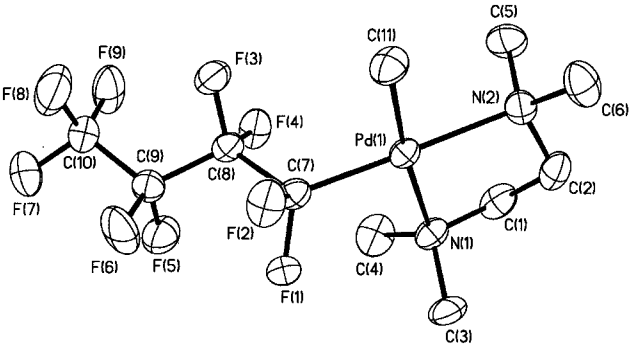

Figure 4. ORTEP diagram of the non-hydrogen atoms of (TMEDA)Pd(CH_3)(*n*-C_4F_9) (**2**), showing atom-labeling scheme. Thermal ellipsoids are shown at the 30% level.

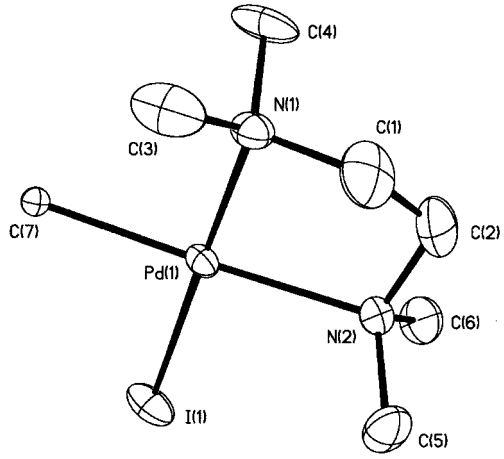

Figure 5. ORTEP diagram of the non-hydrogen atoms of (TMEDA)Pd(CH_3)I (**3**), showing atom-labeling scheme. Thermal ellipsoids are shown at the 30% level.

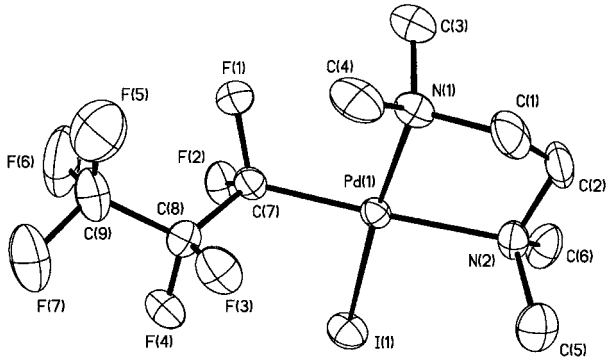

Figure 6. ORTEP diagram of the non-hydrogen atoms of (TMEDA)Pd(*n*-C_3F_7)I (**4**), showing atom-labeling scheme. Thermal ellipsoids are shown at the 30% level.

perfluoro-*n*-propyl ligand, supporting observations previously made in analogous comparisons of CH_3 and CF_3 ligands.[7,26−28] It is of interest to note that the Pd−N distances in analogous nonfluorinated systems show a much narrower range, as shown in Table 2: [((TMEDA)-Pd(CH_3)Ph, 2.195(3) Å, 2.210(3) Å; (TMEDA)Pd(CH_3)$_2$, 2.200(2) Å, 2.197(2) Å]. Despite the variation in the bond lengths, there is relatively little distortion to the square-planar core, as the sum of the angles around palladium (360.1°) indicates a virtually flat structure. A notable observation is that the average α-CF_2 bond angle (F(1)−C(8)−F(2) is significantly more acute at 100.7(7)° compared with that of the β-CF_2 group, where the average F(3)−C(9)−F(4) angle is 105.6(9)°. The angles at carbon down the fluorocarbon chain are quite obtuse, averaging 118.1(7)° for Pd(1)−C(8)−C(9) and 119.6(10) for C(8)−C(9)−C(10).

(TMEDA)PdI(*n*-C_3F_7) (**4**) crystallizes in the triclinic space group $P\bar{1}$ and also contains two crystallographically independent molecules in the asymmetric unit. However, the two molecules are not related by being nonsuperimposable mirror images, but by subtle conformational changes in the CH_2CH_2 backbone and orientational differences in the perfluoropropyl group.

(26) Appleton, T. G.; Clark, H. C.; Manzer, L. E. *Coord. Chem. Rev.* **1973**, *10*, 335−422.
(27) Bennett, M. A.; Chee, H.-K.; Jeffery, J. C.; Robertson, G. B. *Inorg. Chem.* **1979**, *18*, 1071−1076.
(28) Bennett, M. A.; Chee, H.-K.; Robertson, G. B. *Inorg. Chem.* **1979**, *18*, 1061−1070.

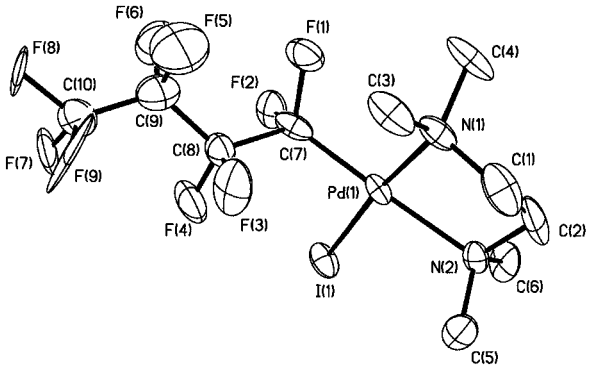

Figure 7. ORTEP diagram of the non-hydrogen atoms of (TMEDA)Pd(*n*-C_4F_9)I (**5**), showing atom-labeling scheme. Thermal ellipsoids are shown at the 30% level. The CF_3 group is arbitrarily shown with one of two rotational orientations.

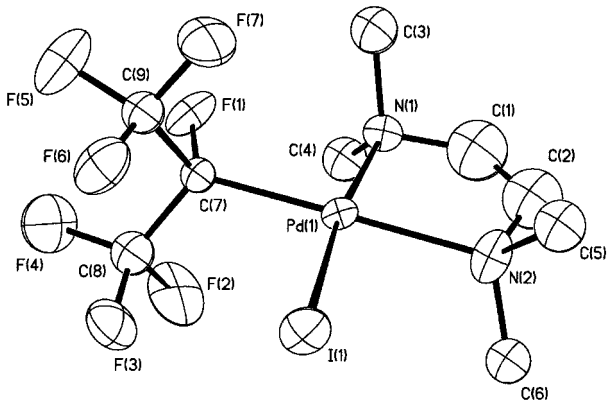

Figure 8. ORTEP diagram of the non-hydrogen atoms of (TMEDA)Pd(*i*-C_3F_7)I (**7**), showing atom-labeling scheme. Thermal ellipsoids are shown at the 30% level.

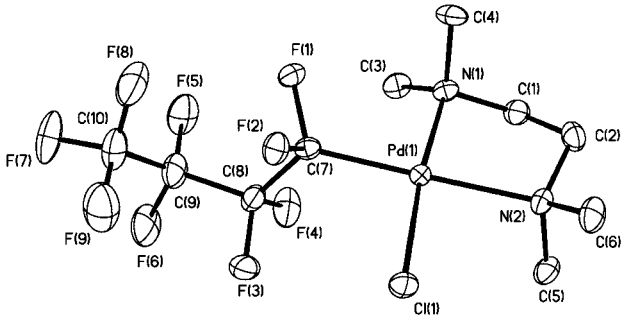

Figure 9. ORTEP diagram of the non-hydrogen atoms of (TMEDA)Pd(*n*-C_4F_9)I (**8**), showing atom-labeling scheme. Thermal ellipsoids are shown at the 30% level.

An ORTEP of one molecule is shown in Figure 4, and an ORTEP showing both molecules is provided in the Supporting Information.

The average Pd−C_F bond distance (2.002(12) Å) is indistinguishable from that in **1**, while the average Pd−I distance (2.5717(14) Å) is similar to that found in (TMEDA)PdPhI (2.5703(8) Å).[25] The length of the Pd−N bond *trans* to the perfluoroalkyl group (Pd−N(2) average 2.165(9) Å) is similar to the corresponding distance in **1**, while the Pd−N bond *trans* to the iodide ligand (2.142(9) Å) is considerably shorter than the analogous bond distance *trans* to CH_3 in **1**, illustrating the weaker *trans*-influence of the iodide ligand relative to the methyl ligand.

The presence of the larger iodide ligand is negligible when considering the steric effect it has on the planarity of the molecule, as the sum of the angles is again 360.1°, identical to that of **1**. This highlights the remarkable flexibility of these molecules and their ability to accommodate ligands of varying steric demand. The same trend of acute bond angles can be observed involving the CF_2 groups; the average angle F(1)−C(7)−F(2) is 103.1(9)° and that of F(3)−C(8)−F(4) is 104.2(9)°, but the difference between individual bond angles F(3)−C(8)−F(4) [106.1(10)°] and F(3′)−C(8′)−F(4′) [102.3(10)°] in the individual molecules indicates that the CF_2 groups may be able to respond in a plastic manner to different forces in the crystal. As observed in **1**, the angles at carbon down the fluorocarbon chain are obtuse, averaging 116.9(7)° for Pd(1)−C(7)−C(8) and 118.7(10) for C(7)−C(8)−C(9).

(TMEDA)Pd(CH_3)(*n*-C_4F_9) (**2**) (Figure 5) crystallizes in the monoclinic space group $P2_1/n$. The Pd−C_F bond distance in **2** (1.990(5) Å) is indistinguishable from the analogous bond distance in **1**, although the Pd−CH_3 bond distance (2.052(5) Å) is slightly shorter than the analogous bond distance of 2.092(10) Å observed for **1**. The Pd−N bond distances are similar to those in **1**: that *trans* to the perfluoroalkyl ligand, Pd(1)−N(2), is 2.167(4) Å and that *trans* to the methyl, Pd(1)−N(1), is 2.235(4) Å. As seen in **1**, the sum of the angles around the metal center (360.1°) indicates little distortion due to the ligands present, and similar patterns of acute F−C−F angles within CF_2 groups and obtuse C−C angles along the fluoroalkyl chain are observed. All of the metrical data for **2** indicate that adding an additional CF_2 group to the perfluoroalkyl chain has little, if any, overall effect on the bonding around the Pd center, or elsewhere in the molecule.

(TMEDA)PdI(*n*-C_4F_9) (**5**) (Figure 6) crystallizes in the monoclinic space group $P2_1/c$. Due to high standard deviations, the Pd−C_F bond distance of 1.943(17) Å is not distinguishable from the analogous bond length determined in **4**, but the Pd−I distance is slightly longer (2.5824(17) Å) than the corresponding distance in **4**. The Pd−N distances are not significantly different from their counterparts in **4** and show the expected differences due to the *trans*-influences of iodide and perfluorobutyl ligands. No significant distortions from planarity around the square-planar palladium are observed, and similar patterns of acute F−C−F angles and obtuse C−C angles are present.

(TMEDA)PdCl(*n*-C_4F_9) (**8**) (Figure 7) crystallizes in the monoclinic space group $P2_1/c$. The Pd−C_F bond distance of 2.002(5) Å is not significantly different from the other primary fluoroalkyl palladium complexes reported here. The Pd−Cl bond distance is 2.2951(13) Å. The relatively weak *trans* influence of the chloride ligand is illustrated by the fact that the bond distance to the nitrogen atom *trans* to the chloride ligand, Pd−N(1), of 2.103(4) Å is shorter than the Pd−N bond distance *trans* to the fluoroalkyl ligand, Pd−N(2), of 2.143(4) Å. Confirmation of the relative *trans*-influences of iodide and chloride by comparing details of this structure with that of its closest counterpart **5** is less satisfactory due the poorer quality of the data for **5**, but the more precise data for the perfluoro-*n*-propyl complex **4** do provide a more meaningful comparison. Not

unexpectedly the Pd(1)−N(1) distance of 2.103(4) Å in **8** is significantly shorter than the analogous distance of 2.142(9) Å in **4**.

(TMEDA)PdI[CF(CF$_3$)$_2$] (7) (Figure 8) crystallizes in the orthorhombic space group *Pca*2$_1$. The structure is the least precise of those reported here, and the relatively high standard deviations, especially those within the fluoroalkyl ligand, preclude some comparisons of distances and angles with those in other molecules containing *n*-perfluoroalkyl ligands. However the Pd−C(7) to the fluoroalkyl carbon is slightly longer than that in **5**, but identical to that in **4**, and the Pd−N(2) distance in **7** is very slightly shorter than those in **4** or **5**. A meaningful comparison of the relative *trans*-influences of *n*-perfluoroalkyl and perfluoroisopropyl ligands is not possible from these data. The angles around Pd sum to 360.2°, indicating no significant deviation from planarity within the square plane of coordination. The steric influence due to the large cone angle of perfluoroisopropyl is manifested by a significantly larger C(7)−Pd(1)−I(1) angle of 93.5(6)° compared with the corresponding value of 89.6(4)° in **4**. However, the most notable feature of the structure is that the TMEDA ring is far less puckered than in the other examples, consistent with the solution NMR behavior discussed previously. A possible reason for this ring flattening is discussed below.

(TMEDA)Pd(CH$_3$)I (3) (Figure 9) crystallizes in the monoclinic space group *P*2$_1$/*n*. While the Pd−I bond distance of 2.5760(14) Å is shorter than the Pd−I bond distances in complexes **4** and **5**, the Pd−C(7) bond distance (2.152(7) Å) is longer than the analogous Pd−C$_{Me}$ bond distances in **1** and **2** and is also longer than those of (TMEDA)Pd(CH$_3$)$_2$ (2.026(3) and 2.029(3) Å) and of (TMEDA)Pd(CH$_3$)Ph (2.107(3) Å). The Pd−N distances show the effects of the relatively strong *trans* influence of the methyl ligand as the bond distance from Pd to the nitrogen atom *cis* to the methyl ligand is 2.120(7) Å, whereas that to the nitrogen atom *trans* to the methyl ligand is 2.204(7) Å. The molecule displays little distortion from a square-planar geometry, as the sum of the angles around the metal mirrors those seen above (360.0°).

Structural Comparisons. The relative steric influences of the ligands are reflected in the C$_F$−Pd−X bond angles. For the perfluoro-*n*-alkyl complexes, when X = methyl, the angles fall in the range 86.8(4)−87.7(4)°, and when X = halide, the angles are slightly larger and fall in the range 89.6(4)−90.2(4)°. The largest C$_F$−Pd−X bond angle is seen in the perfluoro-iso-propyl iodide complex **7** (93.5(6)°). Despite the presence of various ligands of different sizes, the sum of the bond angles about the square-planar Pd center remains constant at 360(1)°.

The degree of puckering of the TMEDA rings in all these compounds can be quantified by defining the least-squares plane containing the Pd and the two N atoms and measuring the distances (rounded to the nearest 0.01 Å) above and below that plane of the two CH$_2$ carbon atoms of the ring backbone. Using this criterion the puckering in the TMEDA rings in compounds **1** (0.35 and 0.26 Å), **2** (0.45 and 0.25 Å), **3** (0.45 and 0.20 Å), **4** (0.40 and 0.28 Å), **5** (0.43 and 0.27 Å), and **8** (0.41 and 0.29 Å) is significant and quite consistent with-

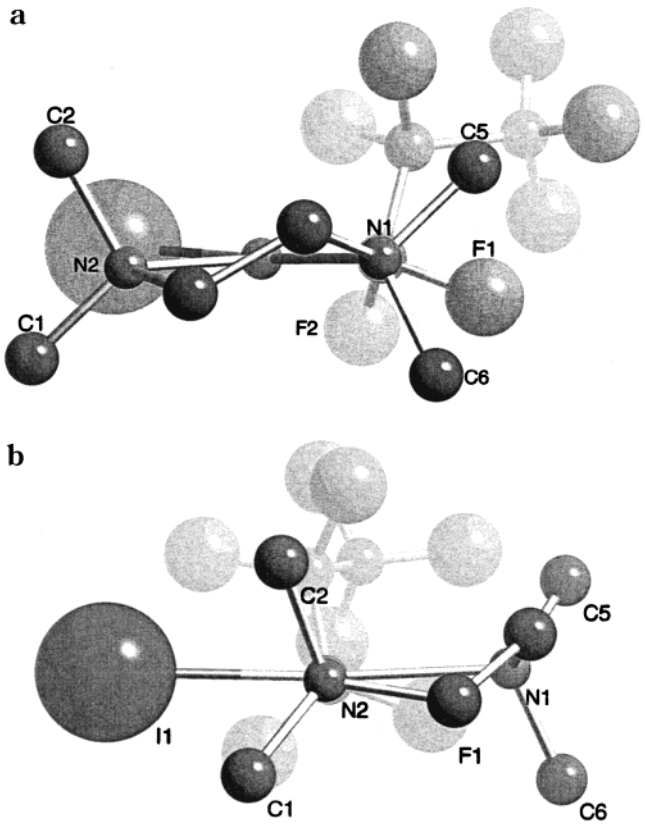

Figure 10. (a) View down the N(1)−C(7) vector in **4** illustrating the staggered conformations of the N(1)Me$_2$ and C$_3$F$_7$ groups. (b) View down the N(2)−Pd−C(7) vector in **4**, illustrating the almost eclipsed conformations of the N(2)Me$_2$ and C$_3$F$_7$ groups.

in the series. The contrast with **7** (0.09 and 0.02 Å), which contains an almost planar TMEDA ring, is dramatic.

The conformational preferences of the TMEDA rings in these complexes can be rationalized in terms of steric interactions. The most direct comparison can be made between the perfluoro-*n*-propyl(iodo) complex **4** and its perfluoroisopropyl isomer **7**. Figure 10a shows a view down the vector connecting the two *cis* atoms N(1) and C(7) of complex **4**; the N(1)−methyl groups and the fluorines and fluoroalkyl group on C(7) adopt the preferred conformation in which these groups are staggered. The pucker of the TMEDA ring follows naturally, to minimize eclipsing interactions, around to N(2), at which point the N(2)−methyl groups are almost perfectly eclipsing the groups on the *trans*-C(7), as shown in Figure 10b. So the avoidance of eclipsing interactions between *cis*-ligand substituents appears to control the conformational preference of the TMEDA ring. The same conformational pattern is found for all the *n*-perfluoroalkyl analogues described here. Contrasting behavior is exhibited by isomer **7**, in which the significantly larger cone angle perfluoroisopropyl ligand[29] appears to possess the dominant steric demand in the coordination sphere. As shown in Figure 11a a view down the C(7)−Pd(1)−N(2) vector illustrates the minimization of steric interactions. The bulky CF$_3$ groups

(29) Hughes, R. P.; Smith, J. M.; Liable-Sands, L. M.; Concolino, T. E.; Lam, K.-C.; Incarvito, C.; Rheingold, A. L. *J. Chem. Soc., Dalton Trans.* **2000**, 873−879.

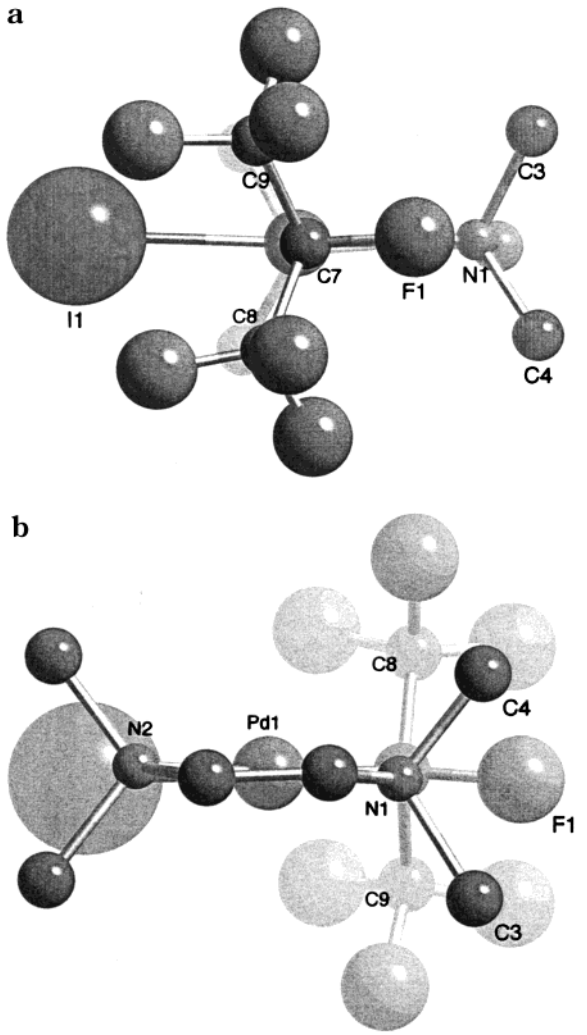

Figure 11. (a) View down the N(2)−Pd−C(7) vector in **7**, illustrating the conformation of the perfluoroisopropyl ligand and the almost eclipsed conformations of the N(2)Me_2 and C_3F_7 groups. (b) View down the N(1)−C(7) vector in **7** illustrating the almost planar TMEDA ring.

lie approximately equally above and below the coordination plane, forcing F(1) into the plane, away from the bulkier *cis*-iodo ligand and toward the less demanding *cis*-N(1)Me_2. In turn, this forces the N(1)−methyl groups out of the pseudoaxial and -equatorial positions favored in **4** (Figure 10), in effect forcing the TMEDA ring to be virtually planar, as shown in Figure 11b. From the NMR studies of ring inversion discussed above, this explains why slowing of inversion of ring pucker in **7** is not observed; it is already planar! Clearly the energetic price of approximately 11−13 kcal mol^{-1} required to flatten the TMEDA ring in solution (vide supra) is paid in the solid state in order to minimize unfavorable steric interactions with the perfluoroisopropyl ligand.

The relative *trans*-influence of ligands bound to square-planar Pd(II) and Pt(II) systems has been the subject of extensive study and review.[26] In general, the relative *trans*-influences of alkyl and fluoroalkyl groups have been determined using spectroscopic rather than crystallographic means. Bennett has made an intermolecular structural comparison of **9** and **10**; the CF_3 analogue of **10** exhibited structural disorder between Cl and CF_3, precluding any meaningful comparison with **9**.[28] The conclusions of this study were that CH_3 has a significantly longer bond to Pt (Pt−C = 2.081(6) Å) in **9** than does C_2F_5 in **10** (Pt−C = 2.002(9) Å), but has a higher *trans*-influence toward Cl (Pt−Cl = 2.412(2) Å) than does C_2F_5 (Pt−Cl = 2.363(2) Å). That the Pt−Cl bond in **10** (and its CF_3 analogue) is indeed stronger than that in **9** is indicated by the values of ν_{Pt-Cl} in **9** (272 cm^{-1}) and **10** (302 cm^{-1}). So the shorter, and

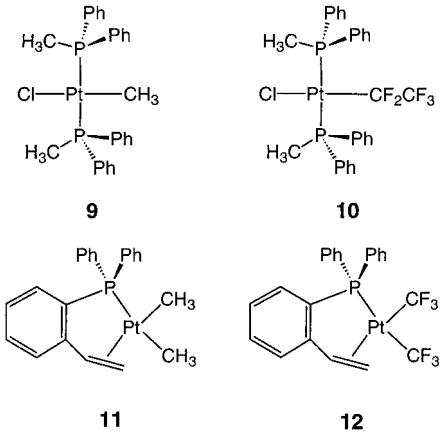

supposedly stronger, bond to the fluorinated carbon atom results in a stronger, shorter bond to the *trans*-Cl.[28] This comparison of the relative *trans*-influences of methyl and perfluoroalkyl ligands *trans* to a potential π-donor ligand (Cl) was complemented by a second structural study of complexes **11** and **12**, each of which contains a pair of Pt−C bonds *trans* to potentially π-acceptor phosphorus and alkene ligands.[27] In these compounds the Pt−CH_3 bond lengths in **11** (2.1665(5) Å *trans* to P; 2.052(6) *trans* to alkene) are longer than the Pt−CF_3 distances in **12** (2.082(5) *trans* to P; 2.032(5) *trans* to alkene), but the corresponding Pt−P (2.276(1) Å) and Pt−alkene (2.223(5) and 2.201(5) Å) bonds in **11** are shorter than the Pt−P (2.310(1) and Pt−alkene (2.290(5) and 2.245(5) Å) bonds in **12**. So the structural *trans*-influences of CH_3 and CF_3 in the latter complexes appear to be reversed from those in **9** and **10**. As Bennett points out,[27] the obvious explanation for both sets of data would be that CF_3 is capable of being a π-acceptor ligand, increasing π-donation from chloride in **10** to strengthen the bond *trans* to itself and competing with the other π-acceptors in **11** and **12** to weaken their respective bonds to Pt. However the idea that CF_3 can act as a significant π-acceptor ligand has fallen into disfavor since MO calculations by Fenske and Hall indicated that this bonding component was of no significance in $(CF_3)Mn(CO)_5$.[30] In addition, a recent valence bond approach to bonding in transition metal complexes suggests that the *trans*-influence may exclusively be attributable to σ-effects.[31] To our knowledge the only previous example of a structure in which it would be possible to obtain an intramolecular comparison of methyl and trifluoromethyl ligands *trans* to the same ligand in the same complex is **13**.[7] Unfortunately the structures of **13** and its dimethyl analogue **14** could not be accurately determined, and the values of all the Pt−alkyl distances in **13** and **14** are indistinguishable

(30) Hall, M. B.; Fenske, R. F. *Inorg. Chem.* **1972**, *11*, 768−775.
(31) Landis, C. R.; Firman, T. K.; Root, D. M.; Cleveland, T. *J. Am. Chem. Soc.* **1998**, *120*, 1842−1854.

at approximately 2.07(2) Å; likewise all the Pt−alkene distances exhibit insignificant differences.

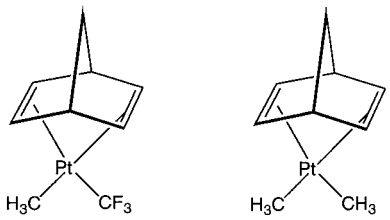

13 **14**

Compounds **1** and **2** described here do allow a direct internal comparison between the *trans*-influences of methyl and fluoroalkyl ligands. The alkyl and fluoroalkyl ligands are each *trans* to the same ligand in a system that is thought to contain no π-acceptor ligands, if we accept the premise that the π-acceptor properties of fluoroalkyl ligands are no better than those of CH_3.[30] If this is indeed true, the differences in bond lengths due to the electronic structures of such complexes are predominantly, if not exclusively, due to σ-effects. It can be seen from the above structural data (Table 2) that the Pd−N bond lengths can be used to determine the relative *trans*-influences of the fluoroalkyl, methyl, and halide ligands, which follow the expected trend methyl > fluoroalkyl > halide.[26] The conclusion from this work is that, relative to the CH_3 ligand, the shorter and presumably stronger Pd−R_F bond gives rise to a shorter and presumably stronger Pd−N bond *trans* to it; that is, R_F possesses a smaller structural *trans*-influence than CH_3 in these compounds. That is, our results parallel those of Bennett on compounds **9** and **10** and contrast, as do his results, with the structural *trans*-influences obtained for **11** and **12**. In further contrast, we have prepared a series of analogous compounds containing platinum in which we can compare N-donor (TMEDA) and P-donor (DMPE) ligands; preliminary structural studies indicate that P-donors show the same trend in bond lengths as N-donors,[32] supporting the idea[31] that π-acceptor properties of ligands are relatively unimportant in determining their *trans*-influences. A more extensive evaluation of crystallographic and spectroscopic properties of these compounds in relation to the *trans*-influences of hydride, alkyl, and perfluoroalkyl ligands is deferred until that work is complete.

Experimental Details

General Considerations. Unless otherwise noted, all reactions were performed in oven-dried glassware, using standard Schlenk techniques, under an atmosphere of nitrogen which had been deoxygenated over BASF catalyst and dried using Aquasorb, or using drybox techniques. THF, diethyl ether, and hexanes were distilled under nitrogen from sodium−potassium alloy benzophenone ketyl, and CH_2Cl_2 from CaH_2, or were dried and degassed over alumina columns under N_2.[33] ^{1}H NMR (300 MHz) and ^{19}F (282 MHz) were recorded on a Varian UNITY plus 300 System in the solvent indicated. Variable-temperature ^{1}H (500 MHz) and ^{19}F (470 MHz) NMR spectra were recorded on a Varian UNITY plus 500 System in the solvent indicated. Chemical shifts were referenced to the solvent peak. Microanalysis were performed by Schwarzkopf Microanalytical Laboratory (Woodside, NY).

Perfluoroalkyl iodides were purchased from Aldrich, treated with $Na_2S_2O_3$ to remove residual I_2, and vacuum distilled before use. (TMEDA)Pd$(CH_3)_2$ was prepared according to a literature procedure.[21]

Reaction of (TMEDA)Pd$(CH_3)_2$ and *n*-C_3F_7I. A. In Hexanes. (TMEDA)Pd$(CH_3)_2$ (0.10 g, 0.40 mmol) was suspended in hexanes (25 mL) in a 125 mL Schlenk flask and stirred vigorously. Neat *n*-C_3F_7I (58 μL) was added, and the resulting mixture was allowed to stir for 12 h. The yellow solid was filtered and extracted into warm hexanes. The combined filtrate and washings were evaporated under vacuum to give pale yellow (TMEDA)PdMe(C_3F_7), **1** (0.10 g, 0.19 mmol), in 48% yield. Anal. Calcd for $C_{10}H_{19}F_7N_2Pd$: C, 29.53; H, 4.71. Found: C, 29.65; H, 4.70. ^{1}H NMR (C_6D_6; 20 °C): δ 2.06 (s, 6H, NMe_2); 1.64 (s, 6H, NMe_2); 1.38 (br s, 4H, CH_2CH_2); 0.66 (br s, 3H, $PdCH_3$). ^{1}H NMR ($CDCl_3$; 20 °C): δ 0.22 (br m, 3H, $PdCH_3$), 2.46 (s, 6H, NMe), 2.55 (s, 6H, NMe), 2.44−2.61 (m, 4H, CH_2). ^{19}F NMR (C_6D_6; 20 °C): δ −79.2 (br s, CF_3); −95.0 (br s, α-CF_2); −117.7 (br s, β-CF_2); $CDCl_3$, δ −79.6 (t, $J_{F\alpha F\gamma}$ = 10 Hz, CF_3), −95.23 (br s, α-CF_2), −118.5 (br s, β-CF_2).

The hexane-insoluble material was determined to be (TMEDA)Pd(CH_3)I, **3** (0.058 g, 0.16 mmol), in 40% yield by comparison of its ^{1}H NMR spectrum with that previously obtained.[21]

B. In THF. (TMEDA)Pd$(CH_3)_2$ (0.10 g, 0.40 mmol) was dissolved in THF (25 mL) in a 125 mL Schlenk flask and stirred vigorously. Neat *n*-C_3F_7I (58 μL) was added, and the resulting yellow mixture was allowed to stir for 12 h, during which time the color became orange. The solution was evaporated under reduced pressure to give an orange solid. This material was extracted into warm hexanes (4 × 10 mL) and thoroughly dried under vacuum to give pale orange (TMEDA)-Pd(C_3F_7)I (**4**; 0.077 g, 0.15 mmol) in 38% yield. Anal. Calcd for $C_9H_{16}F_7IN_2Pd$: C, 20.85; H, 3.11. Found: C, 20.98; H, 3.03. ^{1}H NMR (acetone-d_6; 20 °C): δ 2.90 (br s, 4H, CH_2CH_2); 2.78 (s, 6H, NMe_2); 2.76 (s, 6H NMe_2). ^{19}F NMR (acetone-d_6; 20 °C): δ −80.9 (s, CF_3); −113.0 (br s, β-CF_2). At higher temperatures the α-CF_2 resonance coalesces and appears at δ −95 ppm (see discussion).

The combined hexane washings were evaporated to dryness, yielding a yellow solid determined to be (TMEDA)Pd(CH_3)-(C_3F_7) (**1**; 0.081 g, 0.20 mmol) in 50% yield. The ^{1}H and ^{19}F NMR data matched that presented above.

Preparation of (TMEDA)Pd(C_3F_7)(CH_3) (1). Neat *n*-C_3F_7I (0.20 mL, 1.39 mmol) was added to a solution of (TMEDA)-Pd$(CH_3)_2$ (0.300 g, 1.19 mmol) in THF (20 mL) and the resultant mixture stirred for 16 h to generate an orange solution. All volatiles were removed under vacuum, and the solid residue was suspended in Et_2O (20 mL) and cooled to −30 °C. Addition of (CH_3)MgBr (3.00 M, 0.40 mL, 1.2 mmol), followed by warming to room temperature and stirring for 30 min, gave a pale yellow solution with a pale precipitate. Addition of H_2O (10 mL) and separation of the organic layer, followed by drying over Na_2SO_4, gave a yellow solution which was reduced in vacuo to a yellow solid. The solid was repeatedly extracted into warm hexanes, and the combined filtrates were reduced in vacuo to a yellow solid, (TMEDA)-Pd(C_3F_7)(CH_3) (**1**; 0.436 g, 91%). The product was purified by slow recrystallization from CH_2Cl_2/hexanes. Yield: 0.391 g, 82%. The hexane-insoluble residue was identified as an approximately 1:1 mixture of (TMEDA)Pd(C_3F_7)I (**4**) and (TMEDA)Pd(CH_3)I (**3**).

Preparation of (TMEDA)PdI(C_3F_7) (4). In the air, (TMEDA)Pd(CH_3)(C_3F_7) (**1**; 0.050 g, 0.12 mmol) was dissolved in hexanes (25 mL) in a 125 mL Erlenmeyer flask containing a magnetic stirring bar. Solid I_2 (0.031 g, 0.12 mmol) was added and the solution was stirred vigorously. After 30 min and upon

(32) Sweetser, J. T.; Williamson, A.; Hughes, R. P. Unpublished observations.

(33) Pangborn, A. B.; Giardello, M. A.; Grubbs, R. H.; Rosen, R. K.; Timmers, F. J. *Organometallics* **1996**, *15*, 1518−1520.

complete dissolution of I_2, an orange-yellow precipitate had formed in the purple-brown solution. This mixture was allowed to stir for an additional 2 h, after which time the solid was filtered and washed repeatedly with hexanes (3 × 10 mL). After drying under vacuum, orange (TMEDA)PdI(C_3F_7) (0.047 g, 0.090 mmol) was isolated in 75% yield. The ^{1}H and ^{19}F NMR data matched that reported above.

Reaction of (TMEDA)Pd(CH_3)$_2$ and *n*-C_4F_9I. A. In Hexanes. Using the procedure described above, the following amounts were used: (TMEDA)Pd(CH_3)$_2$ (0.20 g, 0.80 mmol); hexanes (25 mL); *n*-C_4F_9I (110 μL). After workup of the reaction mixture, pale yellow (TMEDA)Pd(CH_3)(C_4F_9) (**2**; 0.20 g, 0.44 mmol) was recovered in 55% yield. Anal. Calcd for $C_{11}H_{19}F_9N_2Pd$: C, 28.93; H, 4.19. Found: C, 29.15; H, 4.30. ^{1}H NMR (C_6D_6; 20 °C): δ 2.05 (s, 6H, NMe_2); 1.63 (s, 6H, NMe_2); 1.36 (br s, 4H, CH_2CH_2); 0.66 (br s, 3H, $PdCH_3$). ^{19}F NMR (C_6D_6; 20 °C): δ −81.2 (s, CF_3); −94.6 (br s, α-CF_2); −113.5 (s, β-CF_2); −125.4 (s, γ-CF_2). At higher temperatures the signal for the α-CF_2 group sharpens considerably (see discussion). ^{19}F NMR (acetone-d_6; −70 °C): δ −80.76 (s, CF_3), −91.72 (d, $J_{F\alpha F\alpha'}$ = 275 Hz, α-CF), −98.68 (d, $J_{F\alpha F\alpha'}$ = 275 Hz, α-CF), −112.12 (d, $J_{F\beta F\beta'}$ = 290 Hz, β-CF), −114.0 (d, $J_{F\beta F\beta'}$ = 290 Hz, β-CF), −124.84 (d, $J_{F\gamma F\gamma'}$ = 290 Hz, γ-CF), −126.18 (d, $J_{F\gamma F\gamma'}$ = 290 Hz, γ-CF). ^{1}H NMR (acetone-d_6; −70 °C): δ 2.13 (s, 3H, NMe), 1.93 (s, 3H, NMe), 1.58 (s, 3H, NMe), 1.46 (s, 3H, NMe), 0.69 (s, 3H, $PdCH_3$; the CH_2 resonances are too broad to observe at this temperature.

The hexane-insoluble material was determined to be (TMEDA)Pd(CH_3)I (**3**, 0.055 g, 0.15 mmol) in 19% yield by comparison of its ^{1}H NMR spectrum to that previously obtained.[21]

B. In THF. Using the procedure described above, the following amounts were used: (TMEDA)Pd(CH_3)$_2$ (0.20 g, 0.80 mmol); THF (25 mL); *n*-C_4F_9I (110 μL). Pale orange (TMEDA)PdI(C_4F_9) (**5**, 0.14 g, 0.25 mmol) was recovered in 31% yield after workup of the reaction mixture. Anal. Calcd for $C_{10}H_{16}IF_9N_2Pd$: C, 21.13; H, 2.84. Found: C, 21.34; H, 2.84. ^{1}H NMR (toluene-d_8): δ 2.10 (s, 6H, NMe_2); 1.91 (s, 6H, NMe_2); 1.24 (m, 4H, CH_2CH_2). ^{19}F NMR (toluene-d_8): δ −81.3 (s, CF_3); −108.4 (s, CF_2); −126.1 (s, CF_2). The α-CF_2 resonance is invisible at this temperature (see discussion). ^{19}F NMR (acetone-d_6; −60 °C): δ −80.75 (s, CF_3), −58.75 (d, $J_{F\alpha F\alpha'}$ = 240 Hz, α-CF), −94.24 (d, $J_{F\alpha F\alpha'}$ = 240 Hz, α-CF), −107.74 (d, $J_{F\beta F\beta'}$ = 289 Hz, β-CF), −109.34 (d, $J_{F\beta F\beta'}$ = 289 Hz, β-CF), −124.25 (d, $J_{F\gamma F\gamma'}$ = 289 Hz, γ-CF), −128.34 (d, $J_{F\gamma F\gamma'}$ = 289 Hz, γ-CF). ^{19}F NMR (acetone-d_6; 80 °C): δ −80.99 (s, CF_3), −74.67 (br s, α-CF_2), −107.93 (s, β-CF_2), −125.34 (s, γ-CF_2). ^{1}H NMR (acetone-d_6; −60 °C): δ 2.48 (s, 3H, NMe), 1.97 (s, 3H, NMe), 1.89 (s. 6H, NMe), 1.75 (m, 1H, CH), 1.67 (m, 1H, CH), 0.64 (m, 1H, CH), 0.52 (m, 1H, CH). ^{1}H NMR (acetone-d_6; 20 °C): δ 2.14 (s, 6H, NMe), 1.98 (s, 6H, NMe), 1.36 (m, 2H, CH_2), 1.30 (m, 2H, CH_2).

The combined hexane washings were evaporated to dryness, yielding a yellow solid determined to be (TMEDA)Pd(CH_3)(C_4F_9) (**2**; 0.16 g, 0.35 mmol) in 44% yield. The ^{1}H and ^{19}F NMR data matched that presented above.

Preparation of (TMEDA)PdI(C_4F_9) (5). In the air, (TMEDA)PdMe(C_4F_9) (**2**; 0.050 g, 0.20 mmol) was dissolved in hexanes (25 mL) in a 125 mL Erlenmeyer flask containing a magnetic stirring bar. Solid I_2 (0.051 g, 0.20 mmol) was added, and the solution was stirred vigorously. After 30 min and upon complete dissolution of I_2, an orange-yellow precipitate had formed in the purple-brown solution. This mixture was allowed to stir for an additional 2 h, after which time the solid was filtered and washed repeatedly with hexanes (3 × 10 mL). After drying under vacuum, orange (TMEDA)PdI(C_4F_9) (0.081 g, 0.14 mmol) was isolated in 70% yield. The ^{1}H and ^{19}F NMR data matched that reported above.

Preparation of (TMEDA)PdCl(C_4F_9) (8). In the air, (TMEDA)Pd(CH_3)(C_4F_9) (**2**; 0.050 g, 0.20 mmol) was dissolved in Et_2O (25 mL) in a 125 mL Erlenmeyer flask containing a magnetic stirring bar. Concentrated HCl (17 μL) was added, and the solution was allowed to stir for 2 h, during which time a yellow precipitate formed. The mixture was filtered and the solid washed with hexanes (10 mL). The wet solid was then dried under vacuum to leave yellow (TMEDA)PdCl(C_4F_9) (**8**; 0.062 g, 0.13 mmol) in 65% yield. Anal. Calcd for $C_{10}H_{16}ClF_9N_2Pd$: C, 25.17; H, 3.38. Found: C, 25.25; H, 3.29. ^{1}H NMR (acetone-d_6, 20 °C): δ 2.98 (br m, 4H, CH_2CH_2); 2.83 (s, 6H, NMe_2); 2.62(s, 6H, NMe_2). ^{1}H NMR (toluene-d_8, 20 °C): δ 2.08 (s, 6H, NMe_2); 1.99 (s, 6H, NMe_2); 1.38 (br m, 4H, CH_2CH_2). ^{19}F NMR (acetone-d_6, 20 °C): δ −82.2 (s, CF_3); −113.2 (s, β-CF_2); −126.8 (s, γ-CF_2). ^{19}F NMR (toluene-d_8, 20 °C): δ −80.9 (s, CF_3); −112.1 (s, β-CF_2); −125.8 (s, γ-CF_2). The α-CF_2 resonance is invisible at this temperature (see discussion). ^{19}F NMR (acetone-d_6; −60 °C): δ −80.74 (s, CF_3), −79.15 (d, $J_{F\alpha F\alpha'}$ = 230 Hz, α-CF), −99.32 (d, $J_{F\alpha F\alpha'}$ = 230 Hz, α-CF), −111.35 (d, $J_{F\beta F\beta'}$ = 295 Hz, β-CF), −113.01 (d, $J_{F\beta F\beta'}$ = 295 Hz, β-CF), −124.81 (d, $J_{F\gamma F\gamma'}$ = 287 Hz, γ-CF), −127.30 (d, $J_{F\gamma F\gamma'}$ = 287 Hz, γ-CF). ^{19}F NMR (acetone-d_6; 80 °C): δ −80.99 (s, CF_3), −87.65 (br s, α-CF_2), −112.01 (s, β-CF_2), −125.16 (s, γ-CF_2).

Reaction of (TMEDA)Pd(CH_3)$_2$ and *i*-C_3F_7I. A. In Hexanes. (TMEDA)Pd(CH_3)$_2$ (0.10 g, 0.40 mmol) was suspended in hexanes (25 mL) in a 125 mL Schlenk flask and stirred vigorously to give a pale yellow mixture. Neat *i*-C_3F_7I (57 μL) was added, and the resulting mixture was allowed to stir for 12 h. The yellow solid was filtered and washed twice with hexanes (15 mL). The combined filtrate and washings were evaporated under vacuum to give pale yellow (TMEDA)Pd(*i*-C_3F_7)(CH_3) (**7**; 0.10 g, 0.19 mmol) in 48% yield. Anal. Calcd for $C_{10}H_{19}F_7N_2Pd$: C, 29.53; H, 4.71. Found: C, 29.56; H, 4.42. ^{1}H NMR (C_6D_6): δ 2.08 (s, NMe_2); 1.58 (s, NMe_2); 1.38 (br m, CH_2CH_2); 0.52 (br s, $PdCH_3$). ^{19}F NMR (C_6D_6): δ −67.1 (s, CF_3); −195.6 (br s, CF).

The hexane-insoluble material was determined to be (TMEDA)Pd(CH_3)I (**3**; 0.058 g, 0.16 mmol) in 40% yield by comparison of its ^{1}H NMR spectrum to that previously obtained.[21]

B. In THF. Addition of *i*-C_3F_7I (0.15 mL, 1.04 mmol) to a colorless solution of (TMEDA)Pd(CH_3)$_2$ (150 mg, 0.594 mmol) in THF (15 mL) gave an orange solution, which was stirred for 16 h to give a deep red solution with a purple suspension. Removal of all volatiles in vacuo followed by extraction into warm hexanes gave a yellow solution, which was reduced in vacuo to a yellow solid, (TMEDA)Pd(*i*-C_3F_7)(CH_3) (**7**; 89 mg, 37%). ^{1}H NMR ($CDCl_3$, 20 °C): δ 0.11 (m, 3H, PdMe), 2.45 (s, 6H, NMe), 2.53 (s, 6H, NMe), 2.40−2.64 (m, 4H, CH_2). ^{19}F NMR ($CDCl_3$, 20 °C): δ −196.2 (septet, 1F, J = 9 Hz, CF), −67.6 (d, 6F, J = 9 Hz, CF_3).

The remaining purple solid was only sparingly soluble in common organic solvents, and ^{1}H NMR spectroscopy revealed a mixture of compounds dominated by a single compound. Recrystallization from CH_2Cl_2 gave large red crystals, which were confirmed by ^{1}H NMR spectroscopy and by elemental analysis to be (TMEDA)PdI_2. Anal. Calcd for $C_6H_{16}I_2N_2Pd$: C, 15.13; H, 3.38; N, 5.88. Found: C, 15.15; H, 3.35; N, 5.83. The volatiles from this reaction were analyzed by GC−MS, and the dominant fate of the perfluoroalkyl group was found to be the hydrofluorocarbon $(CF_3)_2CFH$.

Preparation of (TMEDA)PdI(*i*-C_3F_7) (7). In the air, (TMEDA)PdMe(*i*-C_3F_7) (**6**; 0.050 g, 0.12 mmol) was dissolved in hexanes (25 mL) in a 125 mL Erlenmeyer flask containing a magnetic stirring bar. Solid I_2 (0.031 g, 0.12 mmol) was added, and the solution was stirred vigorously. After 30 min and upon complete dissolution of I_2, an orange-yellow precipitate had formed in the purple-brown solution. This mixture was allowed to stir for an additional 2 h, after which time the solid was filtered and washed repeatedly with hexanes (3 × 10 mL). After drying under vacuum, orange-red (TMEDA)PdI(*i*-C_3F_7) (0.034 g, 0.066 mmol) was isolated in 55% yield. Anal. Calcd for $C_9F_{16}F_7IN_2Pd$: C, 20.85; H, 3.11. Found: C, 20.71; H, 2.97. ^{1}H NMR (acetone-d_6): δ 2.95 (br s, CH_2CH_2); 2.84 (s,

NMe_2); 2.77 (s, NMe_2). ^{19}F NMR (acetone-d_6): δ −65.5 (s, CF_3); −191.4 (br s, CF).

Crystallographic Structural Determinations. Crystal, data collection, and refinement parameters are collected in Table 1. The systematic absences in the diffraction data are uniquely consistent for the reported space groups. The structures were solved using direct methods, completed by subsequent difference Fourier syntheses, and refined by full-matrix least-squares procedures. DIFABS absorption correction was applied to **5** and **7**, while no absorption correction was necessary for **4** and **8**. For **5**, the fluorine atoms F(7), F(8), and F(9) were equally disordered over two positions. Due to the weakness of the diffraction data for **7** and the resulting small number of observed data, only elements heavier than carbon were refined with anisotropic thermal parameters. For other compounds, all non-hydrogen atoms were refined with anisotropic displacement coefficients and hydrogen atoms were treated as idealized contributions

All software and sources of the scattering factors are contained in the SHELXTL (5.10) program library.

Acknowledgment. R.P.H. is grateful to the National Science Foundation and to the Petroleum Research Fund, administered by the American Chemical Society, for generous financial support. Mr. Wayne Casey is thanked for experimental assistance in obtaining the variable-temperature NMR spectra.

Supporting Information Available: Atomic fractional coordinates, bond distances and angles, and anisotropic thermal parameters for **1**, **2**, **3**, **4**, **5**, **7**, and **8** are available free of charge via the Internet at http://pubs.acs.org.

OM000694K